

# Induction of charge density waves by spin density waves in iron-based superconductors

A. V. Balatsky,<sup>1,2</sup> D. N. Basov,<sup>3</sup> and Jian-Xin Zhu<sup>1</sup>

<sup>1</sup>Theoretical Division, Los Alamos National Laboratory, Los Alamos, New Mexico 87545, USA

<sup>2</sup>Center for Integrated Nanotechnology, Los Alamos National Laboratory, Los Alamos, New Mexico 87545, USA

<sup>3</sup>Department of Physics, University of California–San Diego, La Jolla, California 92093, USA

(Received 13 August 2010; revised manuscript received 5 October 2010; published 22 October 2010)

We argue that spin density wave (SDW) phase in ferrous superconductors contains charge density wave (CDW) with the modulation momentum that is a double of characteristic momenta of SDW. We discuss symmetry constraints on allowed momenta of CDW generated by coupling to spin modulations. To be specific, we considered the CDW that could be realized in Fe-11 (e.g., FeTe) and Fe-122 (e.g., BaFe<sub>2</sub>As<sub>2</sub>) compounds. In case of commensurate SDW, the CDW modulation vector is at the Bragg-peak positions and could be revealed by local scanned probes. In case of incommensurate SDW, the CDW is incommensurate and can be seen also by x-ray and elastic neutron scattering. We also discuss observable charge modulation due to CDW formation near defects and twin boundaries.

DOI: [10.1103/PhysRevB.82.144522](https://doi.org/10.1103/PhysRevB.82.144522)

PACS number(s): 74.25.F-, 74.20.De, 74.62.Dh, 74.81.Bd

## I. INTRODUCTION

New class of ferrous superconductors with critical temperatures reaching above 50 K, have become a major subject of current research in superconducting materials. Ferrous superconductors exhibit substantial similarities with high- $T_c$  cuprate oxides: parent stoichiometric compounds are anisotropic, they develop antiferromagnetic (AFM) commensurate order and are nonsuperconducting. Superconductivity sets in or is enhanced when most of these materials are doped, as is the case in cuprates, although there are superconducting pnictides that are stoichiometric.

In ferrous superconductors, normal state is a conducting SDW magnetic state that sets in below fairly high temperatures  $T_{SDW}$  170 K.<sup>1</sup> The AFM order has been predicted by the conventional spin density wave (SDW) nesting along  $(\pi, 0)$  and  $(0, \pi)$ .<sup>2,3</sup> Discovery of the FeTe superconductors has revealed further interesting evolution of SDW from commensurate SDW to incommensurate configuration as a function of Se or Fe doping.<sup>4</sup> Another common aspect between cuprates and iron pnictides is the reduced kinetic energy of charge carriers.<sup>5</sup> The similarities in the behavior of these materials have prompted a lot of discussions on the role of strong correlations in pnictides.<sup>1,6-9</sup>

While similarities are often emphasized, we want to focus on one qualitative difference between these classes of superconductors: SDW state is conducting in Fe based superconductors, normal state is closer to metal. Charges in this state therefore can adjust and rearrange. We therefore want to explore the onset of charge order as driven by SDW. Situation is qualitatively different from cuprates. In cuprates, the onset of incommensurate charge modulation [charge density wave (CDW) or stripes] drives the appearance of the incommensurate spin fluctuations and sometime order.<sup>10</sup> In ferrous materials, we expect that SDW *drives the formation of* CDW. The effect of charge modulation is a consequence of SDW and charge density will develop in addition to whatever ionic displacements occur due to orthorhombic distortions of the crystal.

## II. GINZBURG-LANDAU ANALYSIS FOR THE SDW-DRIVEN CDW

Idea that the CDW is formed due to the SDW is not new. Experimentally, it has been observed in cuprates that in the vortex cores<sup>11</sup> and in zero field<sup>12-15</sup> competing superconducting and SDW orders lead to the SDW that in turn can lead to the CDW formation. Theory predicts that the CDW modulation, induced due to the SDW formation, will be at the multiples of the momentum of the SDW order, as was pointed out by Kivelson and co-workers,<sup>10</sup> and by Zhang and co-workers.<sup>16</sup> This prediction follows from the observation that one can have a SDW-CDW coupling of the form

$$F_{int} = \lambda \rho_{\mathbf{q}} S_{\mathbf{q}_1}^i S_{-\mathbf{q}_1}^j + \text{H.c.}, \quad (1)$$

To preserve overall translational invariance of free energy, the momenta of two SDW fields should add up to match the momentum of induced the CDW order. Charge and spin density modulations are defined as expectations of the respective operators

$$\rho_{\mathbf{q}} = \left\langle \sum_{\mathbf{k}, \alpha} c_{\mathbf{k}+\mathbf{q}, \alpha}^\dagger c_{\mathbf{k}, \alpha} \right\rangle, \quad (2a)$$

$$S_{\mathbf{q}}^i = \left\langle \sum_{\mathbf{k}} c_{\mathbf{k}+\mathbf{q}, \alpha}^\dagger \sigma_{\alpha\beta}^i c_{\mathbf{k}, \beta} \right\rangle, \quad (2b)$$

where  $i=x, y, z$  are the spin components,  $\alpha, \beta$  are spin indices. Ordered state is characterized by the amplitude of SDW and CDW modulations that are now classical field and are smoothly varying in space and in time,

$$\rho_{\mathbf{q}} = \int d\mathbf{r} \rho(\mathbf{r}) \exp(i\mathbf{q} \cdot \mathbf{r}), \quad (3)$$

$$S_{\mathbf{q}}^i = \int d\mathbf{r} S^i(\mathbf{r}) \exp(i\mathbf{q} \cdot \mathbf{r}), \quad (4)$$

and this amplitude will have real and imaginary parts. For the purpose of present discussion, we assume that spin polarization will be along  $z$  axis and all relevant spin fields will

have only  $x$  component,  $i=z$ . We notice that the orientation of spin polarization in the SDW state of pnictides is along the  $x$  direction but our discussion here is general enough.

For any state that does not exhibit a spontaneous CDW transition, the free energy would be quadratic in CDW order parameter  $\rho_{\mathbf{q}}$  with a positive “mass” term

$$F_{\text{CDW}} = \frac{1}{2} \Delta_c |\rho_{\mathbf{q}}|^2. \quad (5)$$

Minimizing the free energy  $F_{\text{CDW}} + F_{\text{int}}$  for the CDW order parameter, one finds that for small CDW modulation, the linear term dominates in the presence of SDW order and thus leads to the CDW order regardless of how large mass term is.<sup>10,16</sup>

$$\rho_{\mathbf{q}} = \frac{\lambda}{\Delta_c} S_{\mathbf{q}_1}^i S_{-\mathbf{q}-\mathbf{q}_1}^i + \text{H.c.} \quad (6)$$

in the presence of a single-domain SDW the only momentum at which SDW order is present is at, say,  $\mathbf{q} = \mathbf{q}_1$ . Then the momentum of second SDW term has to be at the same value:  $\mathbf{q} + \mathbf{q}_1 = -\mathbf{q}_1$ . It follows immediately that CDW modulation will be present at  $\mathbf{q} = \pm 2\mathbf{q}_1$ . Therefore, the only allowed momenta at which CDW can develop will be even multiples of underlying SDW momentum.<sup>10,16</sup> Case discussed to date in context of high- $T_c$  cuprates is the *monodomain* incommensurate SDW that in turn will induce incommensurate CDW.

Parent compound of 122 pnictides as well as 11 compounds forms a *commensurate* SDW,<sup>4,17</sup>

$$\mathbf{q}_1 = (\pi, 0), \quad \mathbf{q}_2 = (0, \pi). \quad (7)$$

The same argument would give the momenta of CDW to be at (modulo reciprocal lattice vectors),

$$\begin{aligned} \mathbf{q}_{\text{CDW}} &= 2\mathbf{q}_1 = (2\pi, 0), \quad 2\mathbf{q}_2 = (0, 2\pi), \\ [\mathbf{q}_1 \pm \mathbf{q}_2] &= (\pi, \pm \pi). \end{aligned} \quad (8)$$

Important difference with the case of cuprates is that in ferrous compounds, the SDW is a robust order with fairly high  $T_N \sim 170\text{--}220$  K. On the other hand, the induced CDW order is soft and presumably is small. Hereafter we will use unfolded Brillouin zone with one Fe atom per unit cell.

The period of the induced CDW is always twice as short as the period of the SDW because for regions with opposite sign of  $S^z \rightarrow -S^z$ , the CDW amplitude would be the same (see Fig. 1). For a single-domain SDW only CDW with commensurate momenta and indistinguishable from the basis lattice vectors is allowed. In practice, there could be domains in SDW order nucleated by defects, imperfections and lattice strains (see Fig. 1). These domains will overlap where two SDW modulations with momenta  $\mathbf{q}_1$  and  $\mathbf{q}_2$  meet. For a multidomain case with long-range domains the new set of CDW momenta emerge, at  $\mathbf{q}_{\text{CDW}} = \mathbf{q}_1 \pm \mathbf{q}_2$  (as demonstrated in Fig. 7 in the later part of the paper). This observation that unique, nontrivial CDW momenta could emerge even for *commensurate* SDW is a main result of this paper. The CDW periodicity is expected to be given by  $2\sqrt{2}$  of the nearest-neighbor Fe-Fe distance, that is 7.9 Å, along (1,1) direction.

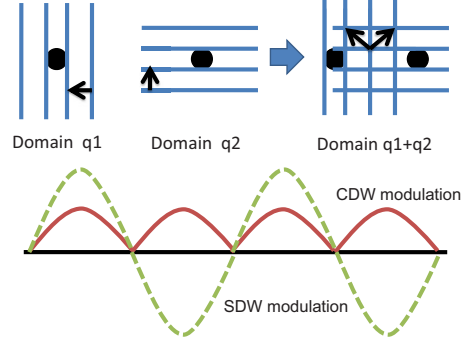


FIG. 1. (Color online) Two domains of SDW that are generated by some defects (black dots) are shown. Periods of SDW are given by reciprocals  $2\pi/\mathbf{q}_1$  and  $2\pi/\mathbf{q}_2$ . In case when the nucleation centers are far there is no overlap and monodomain SDW pattern persists for a long distance. When defects are close by the overlap of the two monodomain SDWs leads to new modulation in spin and as a result in charge density, allowing formation of a new CDW with periods at  $\mathbf{P}_{\pm} = 2\pi/\mathbf{q}_1 \pm 2\pi/\mathbf{q}_2$ . Fourier-transform image of the multidomain CDW would have new peaks at  $\mathbf{Q} = 4\pi/\mathbf{P}_{\pm} = [\mathbf{q}_1 \pm \mathbf{q}_2]$ . Period doubling of CDW with respect to SDW period is illustrated at the bottom.

The SDW transition is well described as a mean-field transition, as seen in experiments. For simplicity we will consider mean-field model in two dimensions (2D) even though the transition in realistic materials is three-dimensional (3D). The effect of magnetic and CDW fluctuations for 3D order and mean-field solutions, we find in 2D are very similar as in both cases we ignore the strong phase fluctuations inherent to two-dimensional models.

To be specific on how the CDW emerge, we use two approaches: Ginzburg-Landau (GL) approach and mean-field model analysis of a microscopic model with the magnetic coupling that mimics spin ordering in ferrous materials. The onset of SDW order leads to nonzero expectation value for the SDW order parameter and is described by GL free energy,

$$\begin{aligned} F_{\text{SDW}} &= C[(\partial_{\mathbf{r}} - i\mathbf{q}_1)S_{\mathbf{q}_1}^i]^2 + (1 \rightarrow 2)] + \frac{1}{2} \alpha_s (T - T_s) [|S_{\mathbf{q}_1}^i|^2 \\ &+ |S_{\mathbf{q}_2}^i|^2] + \frac{1}{4} \beta_1 [|S_{\mathbf{q}_1}^i|^4 + |S_{\mathbf{q}_1}^i|^4] + \frac{1}{4} \beta_2 |S_{\mathbf{q}_1}^i|^2 |S_{\mathbf{q}_2}^i|^2. \end{aligned} \quad (9)$$

Here we assume explicitly that there are two allowed orientations of the SDW domains due to square lattice symmetry with in plane momenta  $\mathbf{q}_1, \mathbf{q}_2$  that are along  $x, y$  axis. Minima for the SDW free energy depend on the ratio of  $\beta_1/\beta_2$ . For  $\beta_1 \geq 2\beta_2$  optimal domain orientation is along  $\mathbf{q}_1 \pm \mathbf{q}_2$ . For the opposite case that we focus on,  $\beta_1 \leq 2\beta_2$  we have the lowest-energy configurations along either  $\mathbf{q}_1$  or  $\mathbf{q}_2$ . Domains are assumed to be large and to extend far beyond the range of defects and imperfections, nucleating them. Hence we will ignore the gradient terms in CDW and SDW free energy. Lorenzana *et al.*<sup>18</sup> have given a detailed analysis of the spin textures and possible charge order within similar

GL approach although they considered only a single-domain textures.

Total free energy is a sum of  $F_{\text{SDW}}+F_{\text{CDW}}+F_{\text{int}}$ . After minimization of the free energy with respect to  $\rho_{\mathbf{q}}, S_{\mathbf{q}}^z$ , the equations for SDW and CDW order are

$$0 = \alpha_s(T - T_s)S_{\mathbf{q}_1}^z + \beta_1|S_{\mathbf{q}_1}^z|^3 + \frac{1}{2}\beta_2|S_{\mathbf{q}_1}^z||S_{\mathbf{q}_2}^z|^2 + \lambda S_{-\mathbf{q}-\mathbf{q}_1}^z\rho_{\mathbf{q}}, \quad (10a)$$

$$0 = \Delta_c\rho_{\mathbf{q}} + \lambda \text{Re}[S_{\mathbf{q}_1}^z S_{-\mathbf{q}-\mathbf{q}_1}^z]. \quad (10b)$$

Solution to Eq. (10b) can be simplified if one notices that  $S^z$  field is the robust dominating order. Hence to first approximation, the first equation can be taken with  $\lambda$  term dropped. This is sufficient for the purpose of proving emergence of distinct CDW. Then in the second equation we will use the unperturbed solution for SDW texture and obtain Eq. (6) with SDW fields having momenta  $\mathbf{q}_1, \mathbf{q}_2$ . CDW component will have the form given by Eq. (6) with

$$\mathbf{q}_{\text{CDW}} = \mathbf{q}_1 \pm \mathbf{q}_2 \quad (11)$$

in addition to doubled momenta  $2\mathbf{q}_1, 2\mathbf{q}_2$ .

### III. MICROSCOPIC MODEL CALCULATIONS FOR THE CDW EMERGING OUT OF THE SDW

To support the analysis of GL approach, we now turn to the microscopic model analysis. We start with a two-band model to include the magnetic interactions for the SDW ordering and its direct coupling to the charge sector,

$$\mathcal{H} = \mathcal{H}_K + \mathcal{H}_M + \mathcal{H}_{\text{int}}. \quad (12)$$

Here the kinetic part is described by

$$\mathcal{H}_K = - \sum_{ij, \alpha\beta, \sigma} (t_{ij, \alpha\beta} + \mu \delta_{ij} \delta_{\alpha\beta}) c_{i\alpha\sigma}^\dagger c_{j\beta\sigma}, \quad (13)$$

where the operators  $c_{i\alpha\sigma}$  ( $c_{i\alpha\sigma}^\dagger$ ) annihilate (create) an electron at the  $i$ th site in the orbital  $\alpha$  and of the spin projection  $\sigma$ . In the numerical calculations, we take the following tight-binding hopping integral parameter values,  $t_1 = -1.0$ ,  $t_2 = 1.3$ ,  $t_3 = t_4 = -0.85$ , and  $\mu = 1.54$ , which appear in the normal-state dispersion in the unfolded Brillouin zone.<sup>19</sup> The part for the SDW ordering is modeled by a spin-exchange interaction term

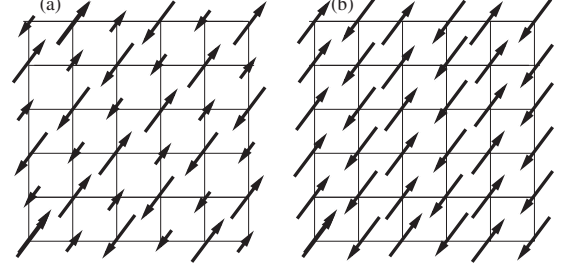


FIG. 2. Schematic in-plane spin structure of (a) Fe-11 and (b) Fe-1111 (or Fe-122) compounds. For Fe-11 systems, the spins are aligned in the form of  $(\uparrow\uparrow\downarrow\downarrow)$  along the  $(1, -1)$  direction in a two-dimensional plane. For Fe-1111 or Fe-122 systems, the spins are aligned in the form of  $(\uparrow\downarrow)$  along the  $(10)$  directions. Perpendicular these specified directions, the spins are aligned ferromagnetically. In each case, two sublattices can be identified.

$$\mathcal{H}_M = \frac{1}{2} \sum_{ij, \alpha} J_{ij} S_{i, \alpha}^z S_{j, \alpha}^z, \quad (14)$$

where  $J_{ij}$  is the magnetic interaction strength. The last term of the total Hamiltonian,  $\mathcal{H}_{\text{int}}$ , describes the interaction between the spin and charge sectors. The form of  $\mathcal{H}_{\text{int}}$  as well as the structure of spin-exchange coupling will be specified below.

We treat the above model Hamiltonian in a mean-field approximation and perform the numerical simulation at zero temperature. Specifically, in the mean-field approximation we start with an initial random distributed spin-polarized electron density that leads to spin configuration  $\langle S_i^z \rangle = \langle n_{i, \uparrow} - n_{i, \downarrow} \rangle$  as an input. After solving mean-field Hamiltonian, we recalculate electron-spin configuration  $\langle S_i^z \rangle$ . The iterative process continues until we reach convergence. At all steps we keep average electron density to be half-filled  $1/N \sum_i \langle n_i \rangle = 2$  by adjusting chemical potential  $\mu$ . The results for respective charge and spin distribution are shown below. We consider in our analysis typical systems of  $40 \times 40$  size.

We consider the case of commensurate magnetic structure as seen in Fe-11 compounds<sup>4</sup> and the case of domain wall between two commensurate configurations. The corresponding magnetic structure for these two cases is shown schematically in Fig. 2.

#### A. Case of $(\frac{\pi}{2}, \frac{\pi}{2})$ SDW

Although the recently discovered Fe(Te,Se) superconductors share the common iron building block and fermiology

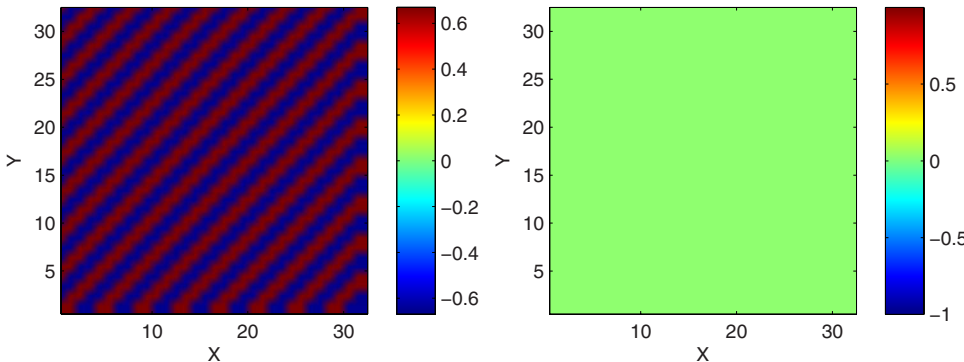


FIG. 3. (Color online) Numerical solution for the spin (left panel) and charge (right panel) profile for  $J_{nn} = 4$ ,  $J_{mnn} = 0$ , and  $g = 0$  for a given orbital, without loss of generality. The spin density is defined as  $M_i = n_{i\alpha\uparrow} - n_{i\alpha\downarrow}$  while the charge density is defined as  $Q_i = n_{i\alpha\uparrow} + n_{i\alpha\downarrow}$ . The right panel shows the relative deviation of the charge density away from its average value.

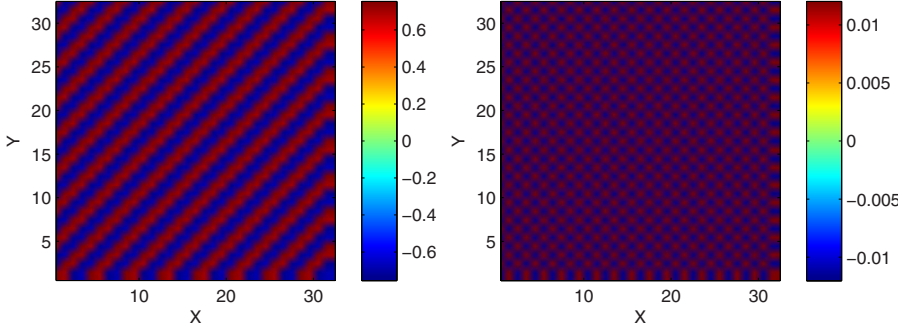


FIG. 4. (Color online) The same as Fig. 3 except for  $J_{nn}=4$ ,  $J_{nnn}=1$ , and  $g=0$ .

with LaFeAsO and BaFe<sub>2</sub>As<sub>2</sub> families of superconductors, the magnetic order is very different from the predicted nesting wave vector  $(\pi, 0)$  and has the ordering wave vector  $(\pi/2, \pi/2)$  [see Fig. 2(a)].<sup>4,20</sup> In these materials, the CDW would be induced even in a single domain of SDW by the same mechanism.

Theoretically, this spin structure can be obtained by choosing the spin-exchange interaction:  $J_{i,i\pm\hat{x}} = \mp J_{nn}(-1)^{i_x+i_y}$ ,  $J_{i,i\pm\hat{y}} = \pm J_{nn}(-1)^{i_x+i_y}$ ,  $J_{i,i\pm\hat{x}\pm\hat{y}} = -J_{nnn}(p)$ , and  $J_{i,i\mp\hat{x}\pm\hat{y}} = J_{nnn}(p)$ , where  $J_{nnn}(p) = J_{nnn}[1 + (1-p)/2]$  with  $p = 1$  for the A sublattice and  $p = -1$  for the B sublattice. Here  $J_{nn}$  and  $J_{nnn}$  represent the nearest-neighbor and next-nearest-neighbor coupling strength. In this case, the coupling between the SDW and CDW orderings can be completely local and modeled as

$$\mathcal{H}_{int} = g \sum_{i,\alpha} n_{i\alpha} S_{i\alpha}^z{}^2 \quad (15)$$

where  $g$  is the coupling strength. In the numerical calculation, we consider a system size of  $N_x \times N_y = 32 \times 32$ .

The results of the solutions for the spin and charge density are shown in Figs. 3–5 for various spin-exchange parameter values and the spin-coupling strength. In the absence of the next-nearest-neighbor exchange interaction ( $J_{nnn}=0$ ) (see Fig. 4), the SDW has the  $(\pi/2, \pi/2)$  pattern. In this case, the magnitudes of the spin-up (or spin-down) magnetic moments on two nearest-neighbor sites are identical while the magnitudes of the spin-up and spin-down magnetic moments are also identical. As such, the CDW is uniform and does not break the translational invariance of an effective two-dimensional Fe square lattice. This is a special case. More generally, the magnitudes of the two spin-up moments can be different. A nonzero  $J_{nnn}$  breaks the degeneracy of SDW magnitudes on two nearest-neighbor sites with the same

spin orientation. Consequently, the charge density on these sites is no longer equal, resulting in a  $(\pi, \pi)$  CDW pattern. The coupling of SDW and CDW ordering can enhance the  $(\pi, \pi)$  CDW pattern (see Fig. 5).

### B. Case for the $(\pi, 0)$ SDW

One way to generate collinear magnetic structure, as shown in Fig. 2(b), is to have opposite signs between the exchange coupling strengths along the  $x$  direction,  $J_{i,i+\hat{x}}$ , and  $y$  direction,  $J_{i,i+\hat{y}}$ , in the homogeneous case. To model multi-domain configuration, we use the ansatz that describes two vertical domains such that for (1)  $i_x < i_{x1}$  and  $i_x < i_{x2}$  or (2)  $i_x > i_{x1}$  and  $i_x > i_{x2}$ ,  $J_{i,i+\hat{x}}$  is positive while  $J_{i,i+\hat{y}}$  is negative, while for (3)  $i_{x1} < i_x < i_{x2}$ ,  $J_{i,i+\hat{x}}$  is negative while  $J_{i,i+\hat{y}}$  is positive. This choice of the spin-exchange coupling guarantees that in the absence of domains, we get the SDW order with wave vector  $(\pi, 0)$  or  $(0, \pi)$ . The above ansatz can be represented by the following formula for the spin-exchange interaction:

$$J_{i,i+\hat{\gamma}} = \pm J_{nn} \tanh[(i_x - i_{x1})(i_x - i_{x2})/\lambda^2]. \quad (16)$$

For the considered system size  $N_x \times N_y = 48 \times 24$ , the positions of domain walls are at  $i_{x1} = 12$  and  $i_{x2} = 36$ . In this case, we consider the spin-charge coupling term as written by

$$\mathcal{H}_{int} = \frac{g}{2} \sum_{ij,\alpha} (n_{i\alpha} + n_{j\alpha}) S_{i\alpha}^z S_{j\alpha}^z \quad (17)$$

with the summation over the spatial sites limited to nearest-neighbor pairs. In the numerical calculations, we take  $J_{nn} = 3$ ,  $\lambda = 2$ , and  $g = 0.2$ .

The results of the mean-field solution for the staggered magnetization and electron-density variation are shown in Fig. 6 with surface [panels (a) and (b)] and image [panels (c)

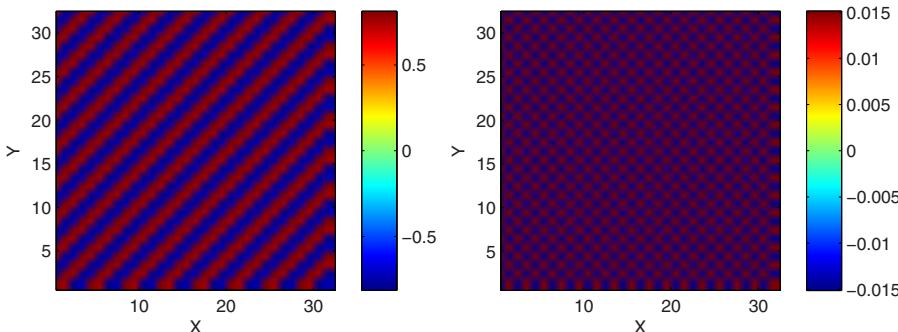


FIG. 5. (Color online) The same as Fig. 3 except for  $J_{nn}=4$ ,  $J_{nnn}=1$ , and  $g=-1.2$ .

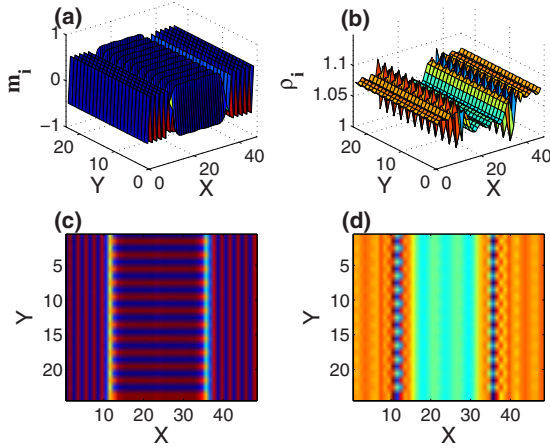


FIG. 6. (Color online) Numerical solution for the spin and charge profile of two monodomains of SDW are shown. (a) The spin profile in two domains. Due to periodic boundary conditions, the regions on both sides of the cell belong to the same domain; (b) the charge profile corresponding to the spin texture on the left; (c) top view of the spin profile. Spin period of the domain on the far left is  $(1,0)$  and the spin period of domain in the middle is  $(0,1)$ ; (d) top view of charge profile related to the spin texture. Emergence of charge modulation and new momenta for charge density modulation are seen near domain walls.

and (d)] plots. The  $(\pi,0)$  and  $(0,\pi)$  SDW order is seen clearly. The zoom-in display of the charge density near the overlap region at the domain wall is presented in Fig. 7 while the charge density along the line cut on the domain wall is shown in Fig. 8. The  $(\pi,\pi)$  charge density modulation is observed near the domain wall.

#### IV. CONCLUDING REMARKS

In conclusion, we propose a mechanism for *commensurate* and *incommensurate* CDW induction due to nonlinear

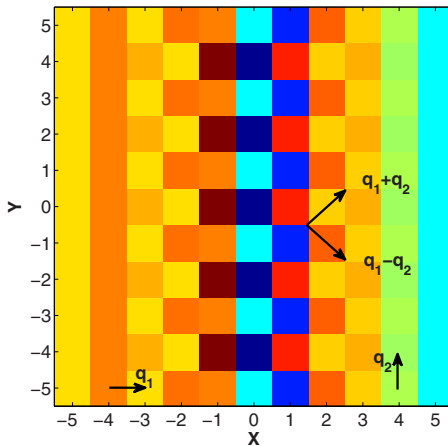


FIG. 7. (Color online) The section of the domain wall is scaled up to show the new periodicity at  $(1,1)$  at the overlap region. We show explicitly respective modulation vectors. The region of new modulation  $q_{CDW}$  will be confined to the overlap region; its size will depend on the thickness of domain wall.

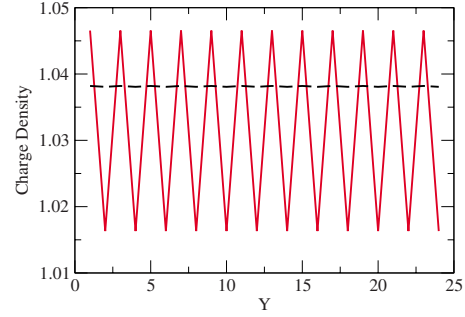


FIG. 8. (Color online) The charge density variation along the domain wall at  $i_x=12$  (red solid line) and deep within the domain wall at  $i_x=24$  (black-dashed) line. The charge density modulation is strongly enhanced near the domain wall.

charge coupling to SDW. For the monodomain SDW state, the momenta of the CDW modulation are trivial and indistinguishable from the main lattice periods. We argue that the multidomain *commensurate* SDW (Ref. 1) can produce observable CDW signatures, such as new peaks in FT STM images and particle-hole asymmetry in local density of states. Recent STM experiments by Niestemski *et al.*<sup>21</sup> have revealed an unusual topographic and spectroscopic signatures for the parent FeAs-122 compound. The required multidomain situation could occur in the presence of strain and defects. Moreover, this situation can be realized in a single-domain FeTe parent compounds where commensurate SDW has been observed. In the case of incommensurate SDW, the induced CDW is incommensurate and hence could be directly seen in scattering experiments, such as neutron and x-ray scattering.

The CDW formation will have experimentally observable consequences: (i) the onset of CDW will occur at the same temperature as SDW state. For specific case of commensurate modulation, CDW modulation will be at the period of  $\sqrt{2} \times a \approx 7.8 \text{ \AA}$ , where  $a$  is the nearest neighbors Fe-Fe distance. (ii) As a result of induced CDW, the new phonon modes will appear as phonon branches would develop new gaps in the folded BZ. The new crossing points of branches then will develop hybridization gaps and the phonon contribution to optical conductivity will reflect these gap openings below SDW transition. These modes also can be seen in low-energy spectroscopy and will have an effect on x-ray and electronic spectra. CDW will also lead to additional partial gapping of electronic spectrum. More detailed analysis that depends on specific material would be required to investigate these effects in details. (iii) CDW amplitude will be proportional to the *square* of the SDW amplitude. The amplitude of CDW modulation will set scale as

$$|\rho_{\mathbf{q}}| \sim |S_{\mathbf{q}_1}^x|^2 \sim |T - T_s|. \quad (18)$$

SDW induced CDW modulation can be observed in spin-unpolarized probes, such as scanning tunneling microscopy (STM) and other probes that couple to charge density. STM would reveal the modulation of particle vs hole states, seen as a particle-hole asymmetry in local density of states with the periodicity set by  $\mathbf{q}_{CDW}$ . STM spectroscopy using

Fourier-transform (FT) STM by Hoffman *et al.*<sup>14</sup> and by Howald *et al.*<sup>15</sup> has been used to observe CDW modulation in cuprates. Similarly, FT STM would be a powerful tool to reveal formation of the new CDW peaks in quasiparticle interference and in topographic images. (iv) We expect that strain in the crystal will play a major role in generating CDW since microscopically the coupling between SDW and CDW, Eq. (1), will occur due to local magnetoelectric coupling. Evidence for strong lattice-magnon coupling in pnictides has been seen in recent Fe isotope experiments.<sup>22</sup> The CDW will be formed in the crystals with the defects and twin or grain boundaries. We note that recent scanning superconducting quantum interference device magnetometry on the twin

boundaries indicate that superfluid density is enhanced near the areas of local strain and frustrated magnetism.<sup>23</sup>

#### ACKNOWLEDGMENTS

We are grateful to S. Kivelson, J. Lorenzana, V. Madhavan, and I. Mazin for useful discussion and for sharing the preliminary STM data. The hospitality of the Aspen Center for Physics (A.V.B.) and the Kavli Institute for Theoretical Physics (A.V.B. and J.-X.Z.) are gratefully acknowledged. This work was supported by U.S. Department of Energy through LDRD and BES funds, the National Science Foundation under Grant No. PHY05-51164, and the UCOP-09-027.

- 
- <sup>1</sup>J. Zhao, W. Ratcliff II, J. W. Lynn, G. F. Chen, J. L. Luo, N. L. Wang, J. Hu, and P. Dai, *Phys. Rev. B* **78**, 140504 (2008).
- <sup>2</sup>F. Ma and Z. Y. Lu, *Phys. Rev. B* **78**, 033111 (2008).
- <sup>3</sup>F. Dong, H. J. Zhang, G. Xu, Z. Li, G. Li, W. Z. Hu, D. Wu, G. F. Chen, X. Dai, J. L. Luo, Z. Fang, and N. L. Wang, *EPL* **83**, 27006 (2008).
- <sup>4</sup>W. Bao, Y. Qiu, Q. Huang, M. A. Green, P. Zajdel, M. R. Fitzsimmons, M. Zhernenkov, S. Chang, M. Fang, B. Qian, E. K. Vehstedt, J. Yang, H. M. Pham, L. Spinu, and Z. Q. Mao, *Phys. Rev. Lett.* **102**, 247001 (2009).
- <sup>5</sup>M. M. Qazilbash, J. J. Hamlin, R. E. Baumbach, L. Zhang, D. J. Singh, M. B. Maple, and D. N. Basov, *Nat. Phys.* **5**, 647 (2009).
- <sup>6</sup>Q. Si and E. Abrahams, *Phys. Rev. Lett.* **101**, 076401 (2008).
- <sup>7</sup>D.-X. Yao and E. W. Carlson, *Phys. Rev. B* **78**, 052507 (2008).
- <sup>8</sup>C. Fang, H. Yao, W.-F. Tsai, J. P. Hu, and S. A. Kivelson, *Phys. Rev. B* **77**, 224509 (2008); K. Seo, B. A. Bernevig, and J. Hu, *Phys. Rev. Lett.* **101**, 206404 (2008).
- <sup>9</sup>I. I. Mazin and M. D. Johannes, *Nat. Phys.* **5**, 141 (2009).
- <sup>10</sup>S. A. Kivelson, I. P. Bindloss, E. Fradkin, V. Oganesyan, J. M. Tranquada, A. Kapitulnik, and C. Howald, *Rev. Mod. Phys.* **75**, 1201 (2003); O. Zachar, S. A. Kivelson, and V. J. Emery, *Phys. Rev. B* **57**, 1422 (1998).
- <sup>11</sup>B. Lake, G. Aeppli, K. N. Clausen, D. F. McMorrow, K. Lefmann, N. E. Hussey, N. Mangkorntong, M. Nohara, H. Takagi, T. E. Mason, and A. Schroder, *Science* **291**, 1759 (2001).
- <sup>12</sup>B. Lake, H. M. Rynn, N. B. Christensen, G. Aeppli, K. Lefmann, D. F. McMorrow, P. Vorderwisch, P. Smeibidl, N. Mangkorntong, T. Sasagawa, M. Nohara, H. Takagi, and T. E. Mason, *Nature (London)* **415**, 299 (2002).
- <sup>13</sup>Y. Kohsaka, C. Taylor, P. Wahl, A. Schmidt, J. Lee, K. Fujita, J. W. Alldredge, J. Lee, K. McElroy, H. Eisaki, S. Uchida, D.-H. Lee, and J. C. Davis, *Nature (London)* **454**, 1072 (2008); Y. Kohsaka, C. Taylor, K. Fujita, A. Schmidt, C. Lupien, T. Hanaguri, M. Azuma, M. Takano, H. Eisaki, H. Takagi, S. Uchida, and J. C. Davis, *Science* **315**, 1380 (2007).
- <sup>14</sup>J. E. Hoffman, E. W. Hudson, K. M. Lang, V. Madhavan, H. Eisaki, S. Uchida, and J. C. Davis, *Science* **295**, 466 (2002).
- <sup>15</sup>C. Howald, H. Eisaki, N. Kaneko, M. Greven, and A. Kapitulnik, *Phys. Rev. B* **67**, 014533 (2003).
- <sup>16</sup>Y. Zhang, E. Demler, and S. Sachdev, *Phys. Rev. B* **66**, 094501 (2002).
- <sup>17</sup>K. Matan, R. Morinaga, K. Iida, and T. J. Sato, *Phys. Rev. B* **79**, 054526 (2009).
- <sup>18</sup>J. Lorenzana, G. Seibold, C. Ortix, and M. Grilli, *Phys. Rev. Lett.* **101**, 186402 (2008).
- <sup>19</sup>S. Raghu, X.-L. Qi, C.-X. Liu, D. J. Scalapino, and S.-C. Zhang, *Phys. Rev. B* **77**, 220503 (2008).
- <sup>20</sup>Y. Xia, D. Qian, L. Wray, D. Hsieh, G. F. Chen, J. L. Luo, N. L. Wang, and M. Z. Hasan, *Phys. Rev. Lett.* **103**, 037002 (2009).
- <sup>21</sup>F. Niestemski, V. Nascimento, B. Hu, W. Plummer, J. Gillett, S. Sebastian, Z. Wang, and V. Madhavan, [arXiv:0906.2761](https://arxiv.org/abs/0906.2761) (unpublished).
- <sup>22</sup>R. H. Liu, T. Wu, G. Wu, H. Chen, X. F. Wang, Y. L. Xie, J. J. Ying, Y. J. Yan, Q. J. Li, B. C. Shi, W. S. Chu, Z. Y. Wu, and X. H. Chen, *Nature (London)* **459**, 64 (2009).
- <sup>23</sup>B. Kalisky, J. R. Kirtley, J. G. Analytis, J.-H. Chu, A. Vailionis, I. R. Fisher, and K. A. Moler, *Phys. Rev. B* **81**, 184513 (2010).